Cluster analysis of acoustic emission signals for 2D and 3D woven glass/epoxy composites

Li Li [a,b], Stepan V. Lomov [b,*], Xiong Yan [a], Valter Carvelli [c]

[a] Key Laboratory of Textile Science and Technology, Ministry of Education, College of Textiles, Donghua University, Shanghai 201600, China
[b] Department of Metallurgy and Materials Engineering, KU Leuven, Kasteelpark Arenberg 44, B-3001 Leuven, Belgium
[c] Department of Architecture, Built Environment and Construction Engineering, Politecnico di Milano, Piazza Leonardo da Vinci 32, 20133 Milano, Italy

1. Introduction

Acoustic emission (AE) registration allows detection of micro-damage events in materials and structures and potentially identification of the damage nature. An acoustic emission signal is an ultrasonic wave resulting from the sudden release of the strain energy when damage happens, for example after fiber breakage, interface debonding, matrix cracking or delamination in composite materials. AE signals contain useful information about the damage mechanisms. The challenge of AE analysis is determining connection between the AE signal parameters and the corresponding damage mode, or discriminating AE signals according to the nature of the damage events they originate from one of the generally accepted ways of discriminating AE signals is cluster analysis, which is a synonym for unsupervised pattern recognition technique [1–8].

In cluster analysis the three important things are [4–6,9]: (1) selection of AE features to be used for cluster definition, (2) choosing the clustering algorithm and (3) validation of the defined clusters.

For the choice of AE features, many descriptors provide rich information about AE signal characteristics, but non-selective use of them may lead to redundancy information for pattern recognition if strong correlation exists among descriptors. Sause [5] made use of an exhaustive search method in feature selection procedure and considered wide range of combinations of signal features extracted from AE signals. For cluster algorithm, the most frequently used methods are k-means, self-organized map combination with k-means and fuzzy-c means algorithm. K-means algorithm is the simplest and effective method for AE signal clustering. Huguet [10], Godin [11], Oliveira [12] and Gutkin [4] used self-organized map combined with k-means to cluster the AE signals.

For investigation of the cluster validity, the most frequently used indexes are Silhouette coefficient [4] and Davies–Bouldin index [9–11]. Sause [5] utilized validation of obtained partitions by cluster validity indices (Davies–Bouldin, Tou indices, Rousseeuw's silhouette validation method and Hubert's Gamma statistics) and voting scheme for the number of clusters with best performance.

Each AE event can be considered as an acoustic signature of one of different damage modes [10]. AE cluster analysis was applied to identification of damage mechanisms in unidirectional glass fiber reinforced polymer (GFRP) in a number of studies [9–11,13–16]. Some authors used time domain features (peak amplitude, duration, rise time, counts, counts to peak and energy) and found that damage mechanisms are highly correlated with peak amplitude. Barre and Benzeggagh [17] give the following peak amplitude

* Corresponding author. Tel.: +32 16 32 12 10; fax: +32 16321990.
E-mail address: stepan.lomov@mtm.kuleuven.be (S.V. Lomov).

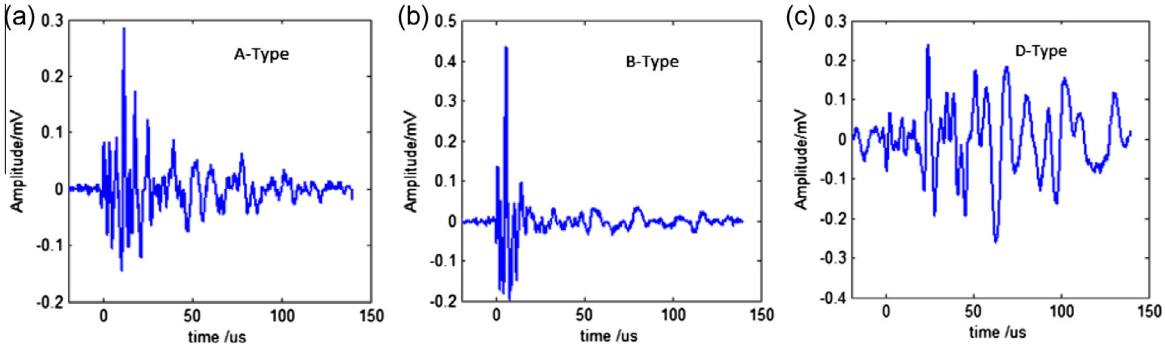

Fig. 1. Typical waveforms for AE signal for glass/epoxy tensile specimens in this study, according to [11]: (a) A-type signal associated with matrix cracking, (b) B-type signals associated with interface debonding, (c) D-type signal associated with delamination.

Table 1
Summary of cluster results in the literature.

AE feature*	Matrix cracking	Debonding	Delamination	Fiber breakage	Fiber pull-out	Materials**	Reference
PA (dB)	40–50	60–65	–	85–95	65–85	G/PP	Barre [17]
	A-type	B-type	–	–	–	G/PET	Huguet [10]
MTF	A-type	B-type	–	C-type	–	G/PET	Godin [9]
	A-type	B-type	D-type	–	–	G/E	Godin [11]
PF (kHz)	30–150	180–290	–	300–400	180–290	G/PET	Suziki [19]
	80–110	230–250	130–200	250–300	–	G/E	Arumugam [13]
AF (kHz)	100–200	210–310	–	330–450	–	G/PET	Pashmforoush [15]
	<50	200–300	50–150	400–500	500–600	C/E	Gutkin [4]

* PA – peak amplitude, PF – peak frequency, AF – average frequency, MTF – multiple time features.
** G – glass fiber, C – carbon fiber, PP – polypropylene, PET – polyester, E – epoxy.

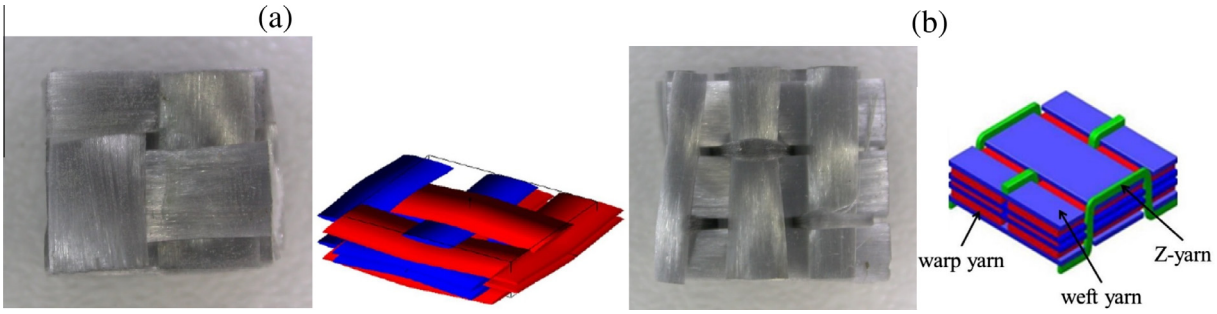

Fig. 2. Internal architecture of (a) 2D plain weave fabric; (b) non-crimp 3D orthogonal weave single-ply preform (fill yarns on the surface, warp yarns underneath them, and *z*-yarns oriented in warp direction over fill yarns). Left: burned-out composite specimens, right: schematic structure of the weave [20].

Table 2
Properties of the preforms: 2D (PW) and 3D [20].

	3D non-crimp woven preform	Plain preform	Weave
	Fabric plies	1	4
	Areal density (g/m^2)	3255	3260
	Insertion density (ends/cm)	2.76	1.95
Warp layer	Top and bottom layer yarns linear density (tex)	2275	2275
	Middle layer yarns linear density (tex)	1100	–
	Insertion density (picks/cm)	2.64	1.6
Fill layer	Yarns linear density (tex)	1470	2275
	Insertion density (ends/cm)	2.76	–
Z yarns	Yarns linear density (tex)	1800	–

ranges for glass/polypropylene composites: 40–55 dB is matrix cracking, 60–65 dB relates to debonding, 65–85 dB relates to fiber pull-out and 85–95 dB is fiber fracture. Peak amplitude related clusters are also described in [9,14,17]. Some researchers [9–11] utilized multiple AE time features for clustering and concluded that there are four typical types of AE signals for GFRP composites. Fig. 1 illustrates three types of them as seen in the experiments reported here for glass/epoxy composites, with interpretation according to [11]: A-type signal associated with matrix cracking with low amplitude, medium rise time and medium duration,

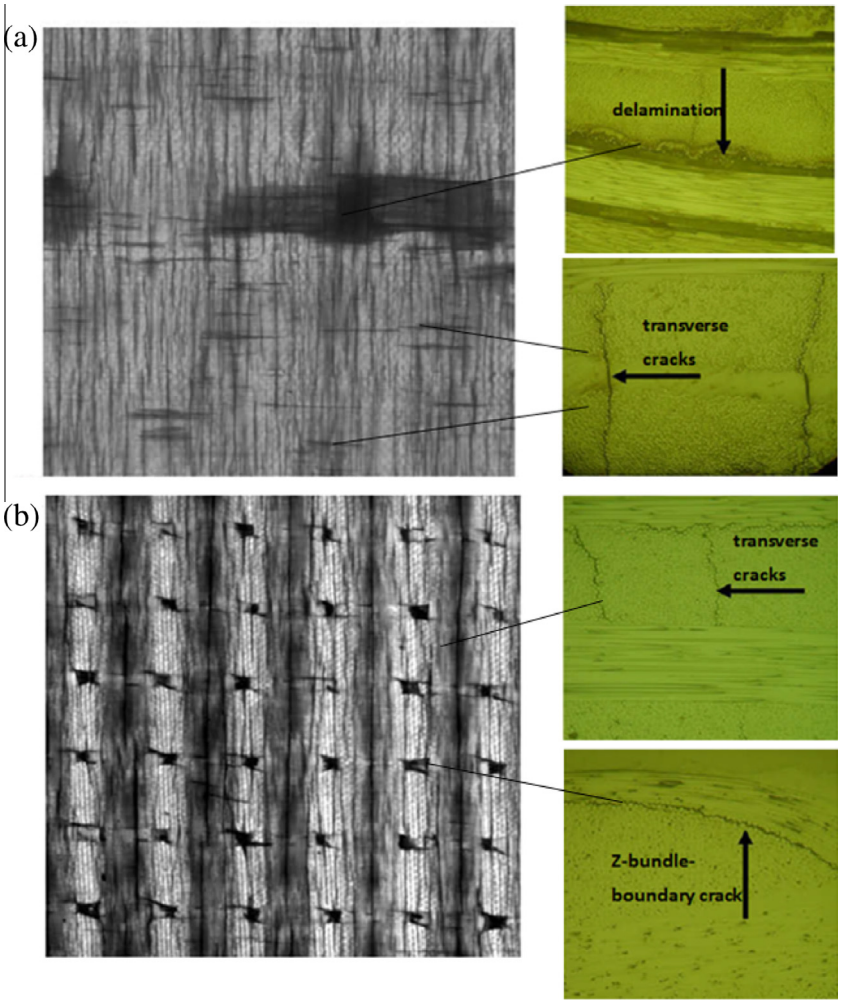

Fig. 3. Transmitting light photos of 2D and 3D composite and micrographs of the same samples (right), loading in the warp direction (horizontal on the images): (a) 2D composite: developed transversal crack in yarns and matrix delamination; and (b) 3D composite, loading in warp direction: transverse cracks and *Z*-bundle-boundary crack [22].

B-type signal related to interface debonding and had short rise time and short duration, D-type signal with medium amplitude, medium rise time and long duration corresponded to delamination in glass/epoxy composites. C-type signals, reported in glass/polyester composites [10] and analogous to B-type, but with much lower amplitude, were not observed in the present study. Ely and Hill [18] showed that in unidirectional graphite/epoxy specimen the stronger signals (high amplitude, energy, counts and long duration) resulted from fiber breakage and the weaker ones (low amplitude, energy, counts and short duration) resulted from longitudinal split cracks. However, this is not supported by the similar observations for glass/epoxy composites.

Some authors used time and frequency features and found that frequency ranges of the clusters are well distinguished, whereas there is an obvious overlap for other parameters [15,16,19]. This leads to a hypothesis that a frequency range is representative of a specific damage mechanism, and frequency can be regarded as the best AE descriptor for damage characterization. Table 1 summaries damage mode links to AE features proposed by different authors for glass fiber reinforced composites.

The materials studied in the present paper are glass/epoxy composites, reinforced with four plies of plain weave E-glass fabric (2D) and single-ply non-crimp 3D orthogonal (3D) E-glass woven fabrics (Fig. 2 and some properties of the preforms in Table 2 [20]). Quasi-static tensile mechanical behavior of 3D woven glass/epoxy composites and their 2D plain weave counterparts, used in the present paper was studied in detail in [21,22], while tensile–tensile fatigue performance was investigated in [20]. For plain weave composites, damage mechanisms include matrix cracking (for the warp direction loading: transverse cracks within fill yarns, longitudinal cracks in the warp direction) and delamination (see Fig. 3(a)). Damage evolution of 3D composite is different because the warp and fill layers are interlaced by *z*-yarns through thickness. The presence of *z*-yarns affects the position and the type of induced damage. For 3D textile composites loaded in the warp direction, there are bundle-boundary cracks on *z*-yarns, transverse cracks in fill direction, cracks in *z*-yarns, cracks in warp yarns (seen Fig. 3(b)). A similar damage pattern was observed for the fill direction loading. For both 2D and 3D glass woven composites, the following damage types can be identified on the intra-ply scale level: (1) matrix intra-yarn cracks, including transverse cracks on yarn boundary, transverse cracks inside yarns, debonding on the yarn surface parallel to the loading; (2) matrix inter-yarn cracks including transverse and longitudinal matrix cracks in matrix pockets, and (3) fiber failure. On the intra-ply level, delamination appear on later stages of the loading.

AE was recorded during these tests, but was analyzed in [21,22] using only the cumulative energy of the AE events. In the present work the clustering analysis is performed on the AE data registered in an independent series of tests performed during the fatigue study of the same materials [20,23]. The synopsis of the paper content is as follows: four AE features were selected after the

Table 3
Acquisition parameters of the AE equipment.

Acoustic emission	Parameters
Software	Vallen AMSY-5
Amplifier	Vallen AEP4
Amplification, dB	34
Discrimination time, ms	0.4
Rearm time, ms	3.2
Range, MHz	0.025–1.6
Sample rate, MHz	5
Sensors	Digital wave B-1025
Sensor diameter, cm	0.93

correlation analysis and Laplacian score criteria from the primary nine AE features, and further narrowed to two: peak amplitude and peak frequency of the signal for the cluster analysis. For all specimens the repeatability of AE events peak amplitude and peak frequency shows that the selected features are uniform for all tensile tests. Then k-means++ clustering algorithm and the principal component analysis were used for cluster the AE events for all specimens. The cluster bonds are identified for the two materials (2D and 3D woven) and different loading directions (warp and fill), and generalized AE cluster structure is presented and possible relation of the clusters to the damage types is hypothesized. These results create a foundation for establishment of general AE interpretation rules for damage mode identification in the future work.

2. Cluster analysis methods

Feature selection is a procedure of extracting the features which are good for classification. 'Good features' are such that objects from the same class have similar feature values and objects from different classes have different values. The goal of feature selection is to find the subset of parameters which eliminate irrelevant and redundant features while keeping relevant features in order to improve clustering efficiency and quality. Existence of irrelevant features in the data set may degrade clustering quality and consume more memory and computational time. In addition, different subset of relevant features may produce different clustering, which will greatly help discovering different hidden patterns in the AE

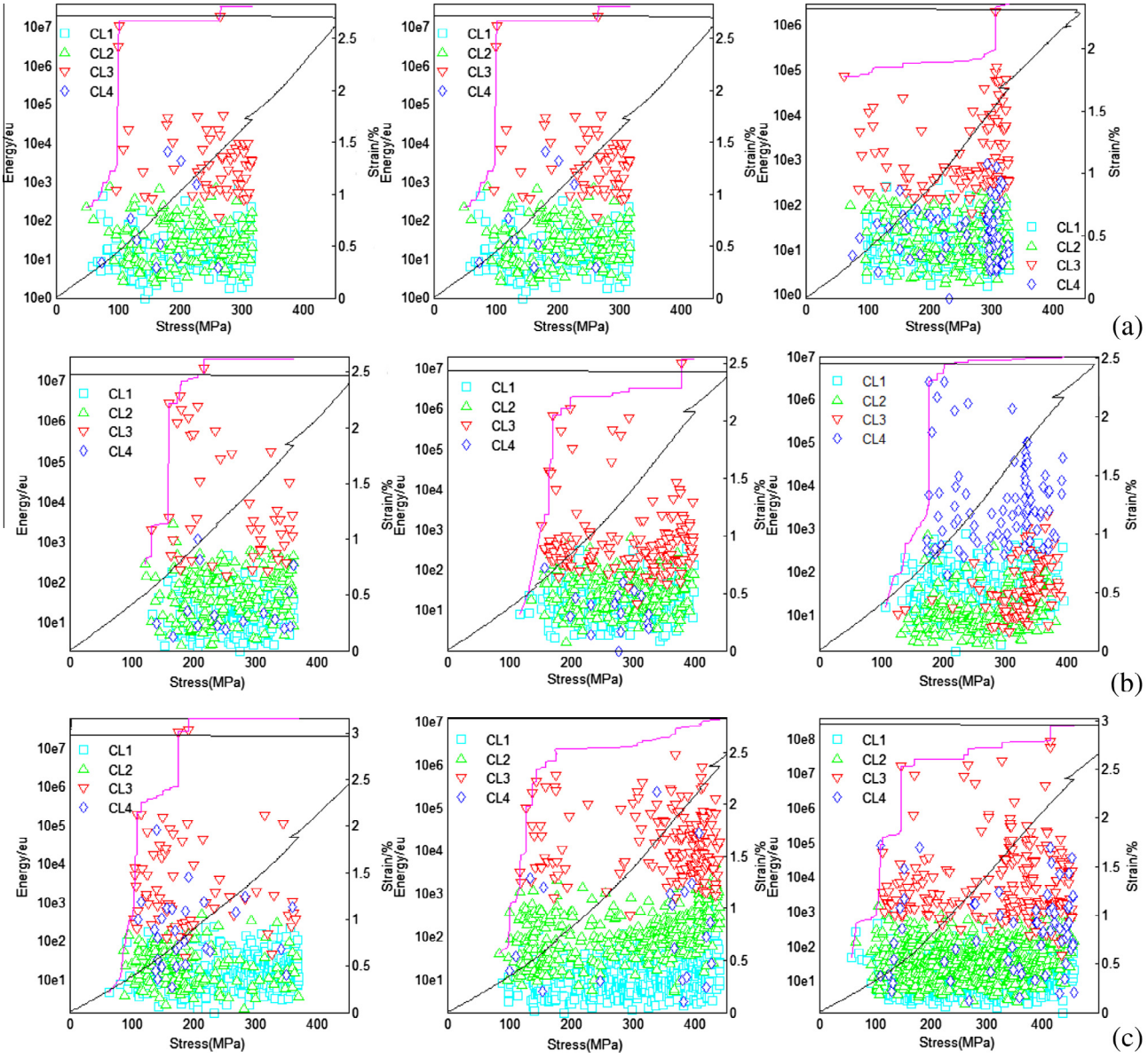

Fig. 4. AE registration events pattern and stress–strain diagrams for all individual tests in (a) PW-1, -2, -3, (b) 3W-1, -2, -3 and (c) 3F-1, -2, -3. The markers represent AE events, classified using the k-means++ algorithm.

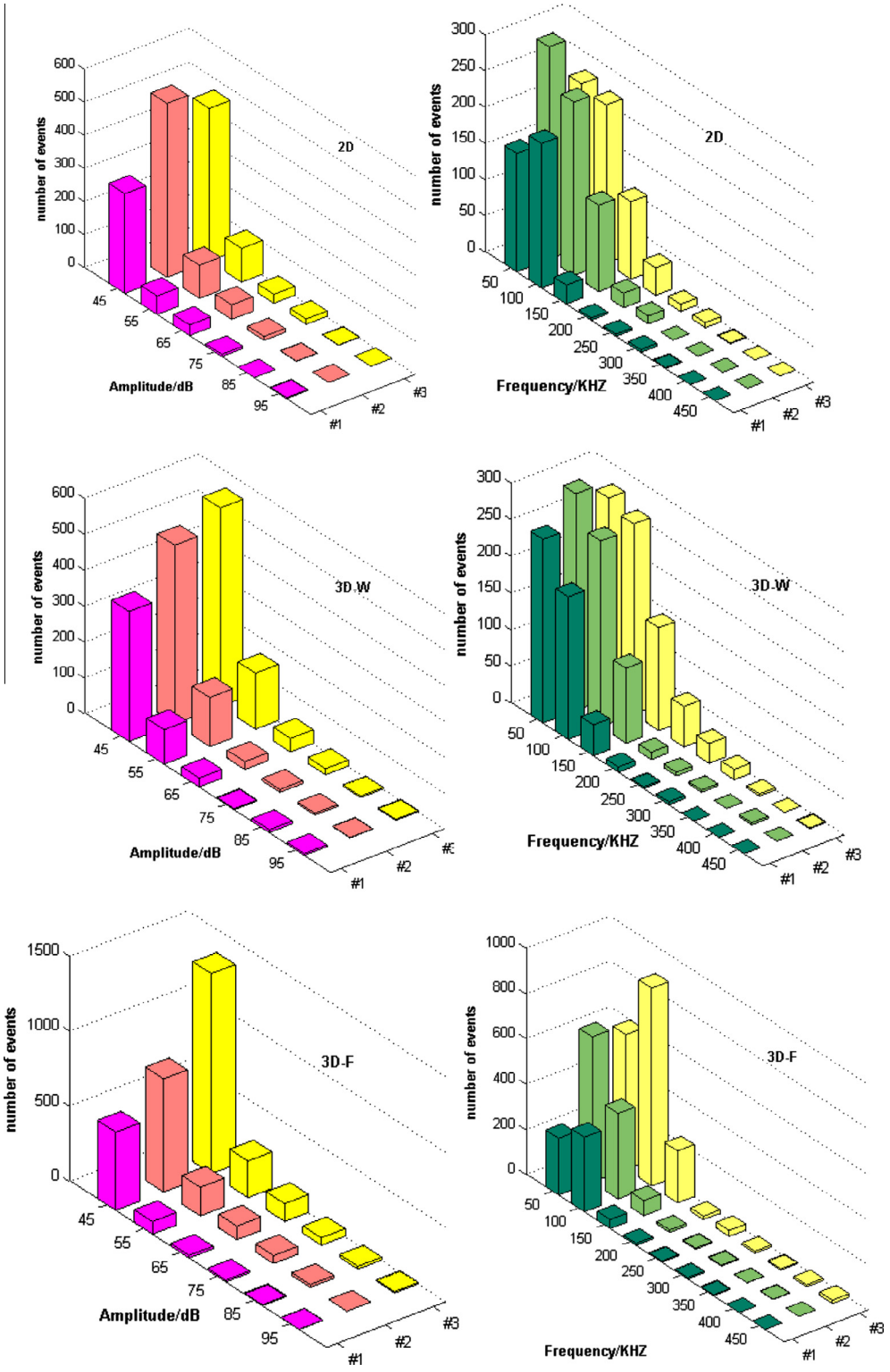

Fig. 5. Distribution of AE events amplitude for individual tests of 2D (PW), 3D-warp (3W) and 3D-fill (3F).

data [24]. For unsupervised feature selection there exist the following methods: maximum variance, Laplacian score, spectral feature selection method and multi-cluster feature selection method. Laplacian score [25,26] it is an advanced variance analysis. It not only prefers those features with larger variances which have more representative power, but also prefers selecting features with stronger locality preserving ability. A key assumption in Laplacian score is that data from the same class are close to each other. Here algorithms from [25] are used to calculate the value of Laplacian score for each feature.

Principle component analysis (PCA) is an orthogonal linear transformation that can transform multidimensional AE data into lower dimensions with a new coordinate system, with a set of uncorrelated features, that is, the principal components [27]. It is an effective and useful multivariate analysis method which is usually used to reduce dimensionality of a large data set to enable

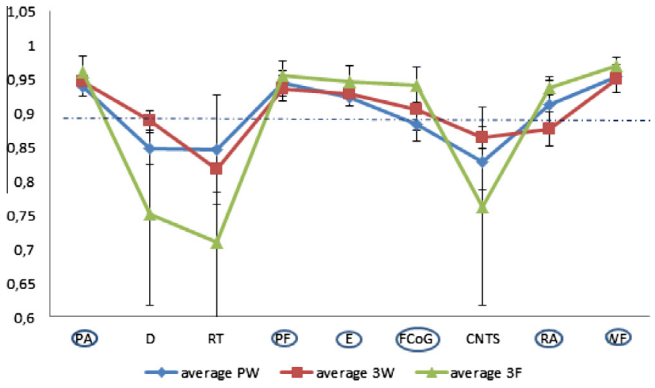

Fig. 6. Feature selection using average and standard variance Laplacian score for all tested specimens PW, 3W, 3F. Error bars indicate standard deviation in three tests. AE features with Laplacian score more than 0.9 in the circles indicate that they have the cluster ability.

better analysis and visualization of data [14,15]. PCA projects the input data (AE signal parameters) on the new coordinates (called principal components) with maximum variance in the data set. Based on the covariance matrix of the dataset the ordered orthogonal basis is created, with its first eigenvectors having the direction of the largest variance of the data. Let A be the matrix, composed of these eigenvectors, then the principal components are expressed as $Pd_i = \sum a_{ij}\bar{p}_j$, where $\bar{p}_j$ are the initial set of the normalized AE signal parameters.

K-means++ [28] is a modified way of choosing centers for the k-means algorithm, which is a centroid based and an iterative algorithm. It follows a simple and easy way to classify a given data set through a certain k number of clusters fixed a priori, in which k centroids are spread throughout the data and the data samples are allocated to the centroid which is closest. Let $D(x)$ denote the shortest distance from a data point to the closest center we have already chosen. Then k-means++ initiation algorithm was defined as follows. Firstly, choose a center at random (uniform distribution) from among the data points. Then compute $D(x)$ for each data point x, make sure that the distance between x and the nearest center has been chosen. After that, use weighted probability distribution $\frac{D(x)^2}{\sum_{x\in\chi} D(x)^2}$ to choose one new data point at random as a new center, which satisfy that its probability proportional to $D(x)$, where χ is the input data set. Repeat the last two steps until k centers have been chosen.

In this study we use two clustering evaluation indices, which are the mostly used in literature: Silhouette coefficient [4] and Davies–Bouldin index [11,29,30]. Silhouette coefficient combines

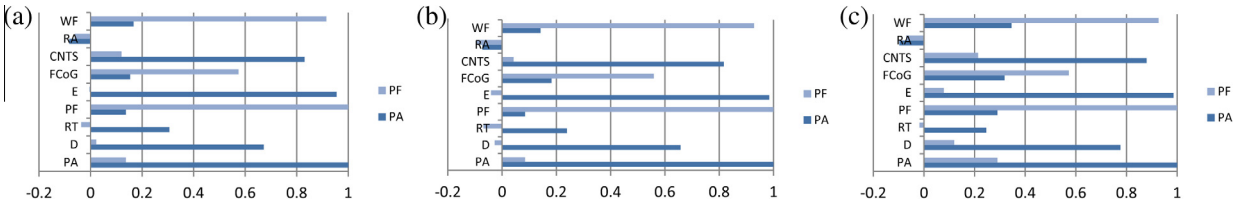

Fig. 7. Correlation coefficient of AE parameters with PA and PF for representative specimens of (a) PW-2, (b) 3W-2 and (c) 3F-1 test variants.

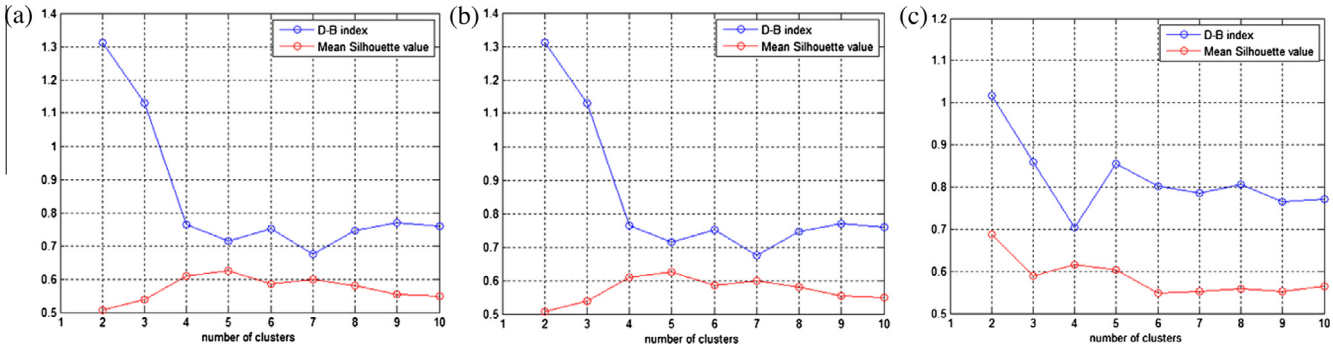

Fig. 8. The number of clusters evaluated by Silhouette coefficient and Davies–Bouldin index: (a) PW, (b) 3W, (c) 3F. Average values in three tests.

Table 4
Four groups clustered by k-means++ for all specimens.

Samples	No. of events	*SC*	DB index	Percentage of events in each cluster			
				CL1	CL2	CL3	CL4
PW-1	399	0.588	1.070	0.451	0.373	0.150	0.025
PW-2	682	0.623	0.794	0.449	0.333	0.163	0.063
PW-3	607	0.611	0.740	0.413	0.315	0.165	0.107
3W-1	499	0.608	0.686	0.459	0.415	0.094	0.032
3W-2	671	0.595	0.855	0.423	0.341	0.212	0.024
3W-3	771	0.606	0.677	0.310	0.453	0.123	0.114
3F-1	643	0.608	0.842	0.579	0.274	0.103	0.045
3F-2	1108	0.616	0.762	0.500	0.336	0.146	0.018
3F-3	1775	0.544	0.866	0.463	0.379	0.123	0.037

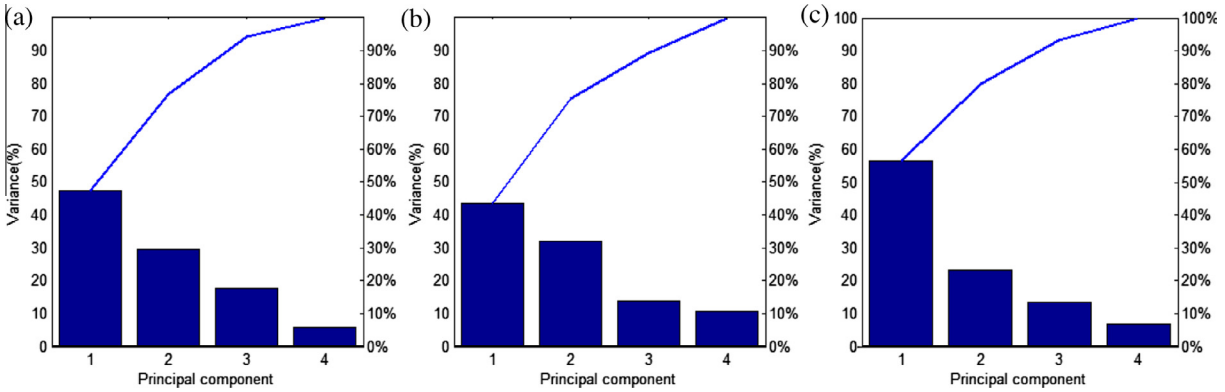

Fig. 9. The variance of principal components of specimens: (a) PW-2, (b) 3W-2 and (c) 3F-1. The *y* axis on the right side shows the cumulative variances (a line in the graphs).

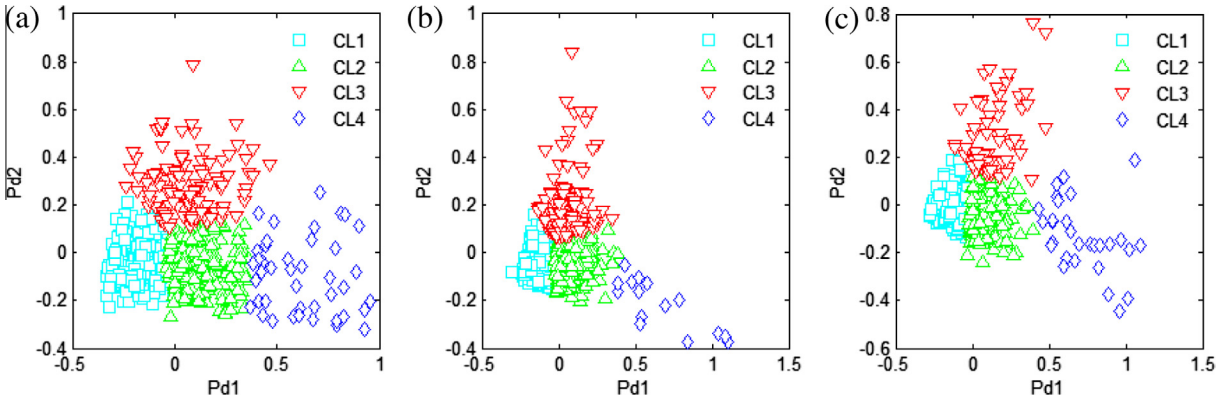

Fig. 10. PCA visualization of k-means++ clustering of textile composites: (a) PW-2, (b) 3W-2, (c) 3F-1.

ideas of both cohesion and separation. It measures how distinct or well-separated a cluster is from other clusters. The Silhouette coefficient for an individual point is given by

$$SC = \frac{1}{N}\sum_{i=1}^{N}\frac{b(x)-a(x)}{\max\{a(x),b(x)\}} \tag{1}$$

where $a(x)$ is the average distance of point x to all other vectors in the same cluster, it measures how closely related are objects in a cluster, $b(x)$ is the average distance of point x to the vectors in other clusters and it aims to find the minimum among the clusters. SC is between -1 and 1. The score is higher when clusters are dense and well separated, which relates to a standard concept of a cluster.

The Davies–Bouldin criterion is based on a ratio of within-cluster and between-cluster distances:

$$\mathrm{DB} = \frac{1}{k}\sum_{i=1}^{k}\max\{D_{i,j}\}, \quad D_{i,j} = \frac{\bar{d}_i + \bar{d}_j}{d(c_i,c_j)} \tag{2}$$

where $D_{i,j}$ is the within-to-between cluster distance ratio for the ith and jth clusters. In mathematical terms, $\bar{d}_i$ is the average distance between each point in the ith cluster and the centroid of the ith cluster. $\bar{d}_j$ is the average distance between each point in the ith cluster and the centroid of the jth cluster. $d(c_i,c_j)$ is the Euclidean distance between the centroids of the ith and jth clusters. The maximum value of $D_{i,j}$ represents the worst case within-to-between cluster ratio for cluster i. The clustering algorithm that produces a collection of clusters with the smallest Davies–Bouldin index is considered the best algorithm based on this criterion. Both Silhouette coefficient and Davies–Bouldin index combine cohesion and separation, but Davies–Bouldin index related to the cluster centroids.

In the present work the cluster analysis is performed based on MatLab R2013a routines from Statistics toolbox.

3. AE data of 2D and 3D woven glass/epoxy composites

3.1. Typical AE registrations and AE signal parameters

In this study acoustic emission data of 2D and 3D glass/epoxy woven composites recorded in the previously reported experiments [23,20] is used. Vallen-5 AE acquisition software was used, with the parameters shown in Table 3. Papers [21,22] report a comparative study of the mechanical properties and damage observation for the two type of materials here considered: four-ply plain weave laminates and single-ply 3D glass non-crimp orthogonal woven composite, which were prepared in the same condition by same processing method and have similar fiber volume fraction and thickness. Because of symmetry of the plain weave laminate there are three set of specimens for loading in the fiber direction were considered: plain weave composite in warp or fill (equivalent) direction (PW), 3D woven composite in warp (3W) and fill (3F) directions. For each variant, three specimens were tested in tension, marked below as PW-1, 2, 3; 3W-1, 2, 3 and 3F-1, 2, 3. The reader is referred to [20,23] for details of the experimental procedure and mechanical test results. Here we concentrate on the cluster analysis of the AE signals.

According to [5,9,11,14,15], nine originally recorded AE features were used to start the clustering analysis (1) peak amplitude (PA), (2) duration (D), (3) rise time (RT), (4) peak frequency (PF), (5) counts (CNT), (6) energy (E), (7) frequency centroid of gravity (FCoG, which is the frequency where the areas of the frequency

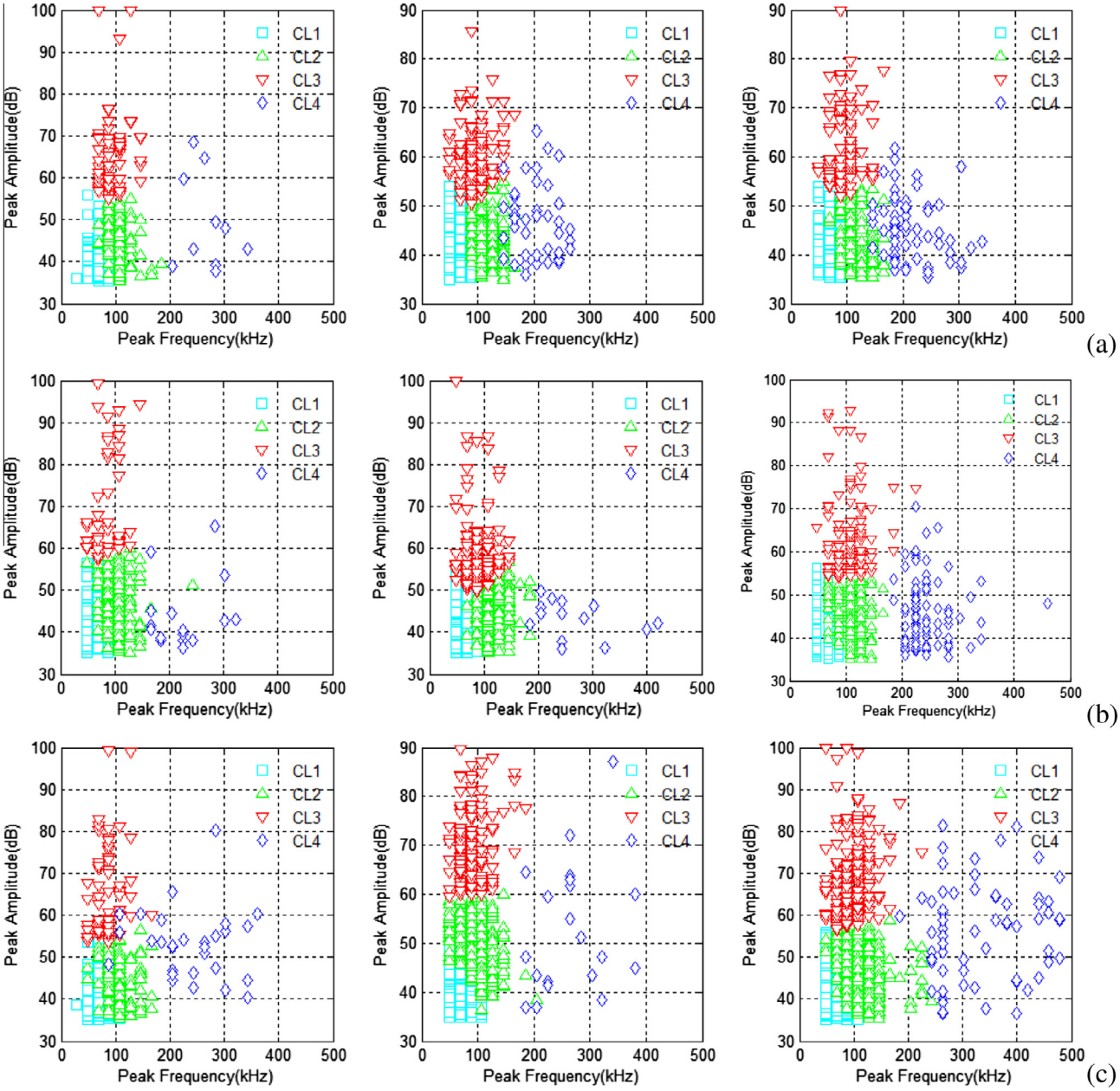

Fig. 11. Cluster results separated by PA and PF for all specimens: (a) PW-1, -2, -3; (b) 3W-1, -2, -3; (c) 3F-1, -2, -3.

spectrum below and above the FCOG are the same), (8) RA value (rise time divided by peak amplitude) and (9) weighted peak frequency (WF, which is square root of peak frequency multiplied by the frequency centroid of gravity). All AE features are normalized to range from 0 to 1 before data analysis.

Fig. 4 presents AE registration data for all PW, 3W and 3F woven tests, together with strain–stress relationship in the same graph. Throughout the paper stress values will be used as the main reference parameter of the loading progression, as the stress values are directly calculated from the specimen load, fed from the Instron machine to AE system and hence are guaranteed to be synchronized. The mechanical behavior of the 2D and 3D specimens is similar (non-linearity of strain–stress diagram, similar pattern of AE energy plot). An important difference between 2D and 3D materials is certain delay (stress difference of 20,...,50 MPa) of initiation of AE activity and the corresponding damage progression in 3D composites in comparison with their 2D counterpart. Fig. 4 also shows grouping of the AE events by clustering, explained later in this paper.

3.2. Repeatability of AE data

The repeatability of AE events for different specimens is shown in Figs. 4 and 5. The data show that AE energy and amplitude pattern is qualitatively stable for 2D and 3D composite in warp and fill direction tests.

For all the three PW specimens, most of the AE events have energy lower than 10e5, there are only one to three relatively high energy events which are more than 10e6, and they are obviously separated by an energy band of 10e5–10e6. For 3D warp direction textile specimens, there are fewer events in the band of 10e3–10e5 than 2D warp direction tests, but it have more events between 10e5 and 10e6. In the fill direction test specimens, there are no such an obvious separation. It is interesting to see that for all the 3D tests, relatively moderate energy from 10e3 to 10e5 are more likely to happened in the lower stress and higher stress, there is a blank existing in the energy spectrum in the moderate load. This AE energy patterns correspond to overall observation of less

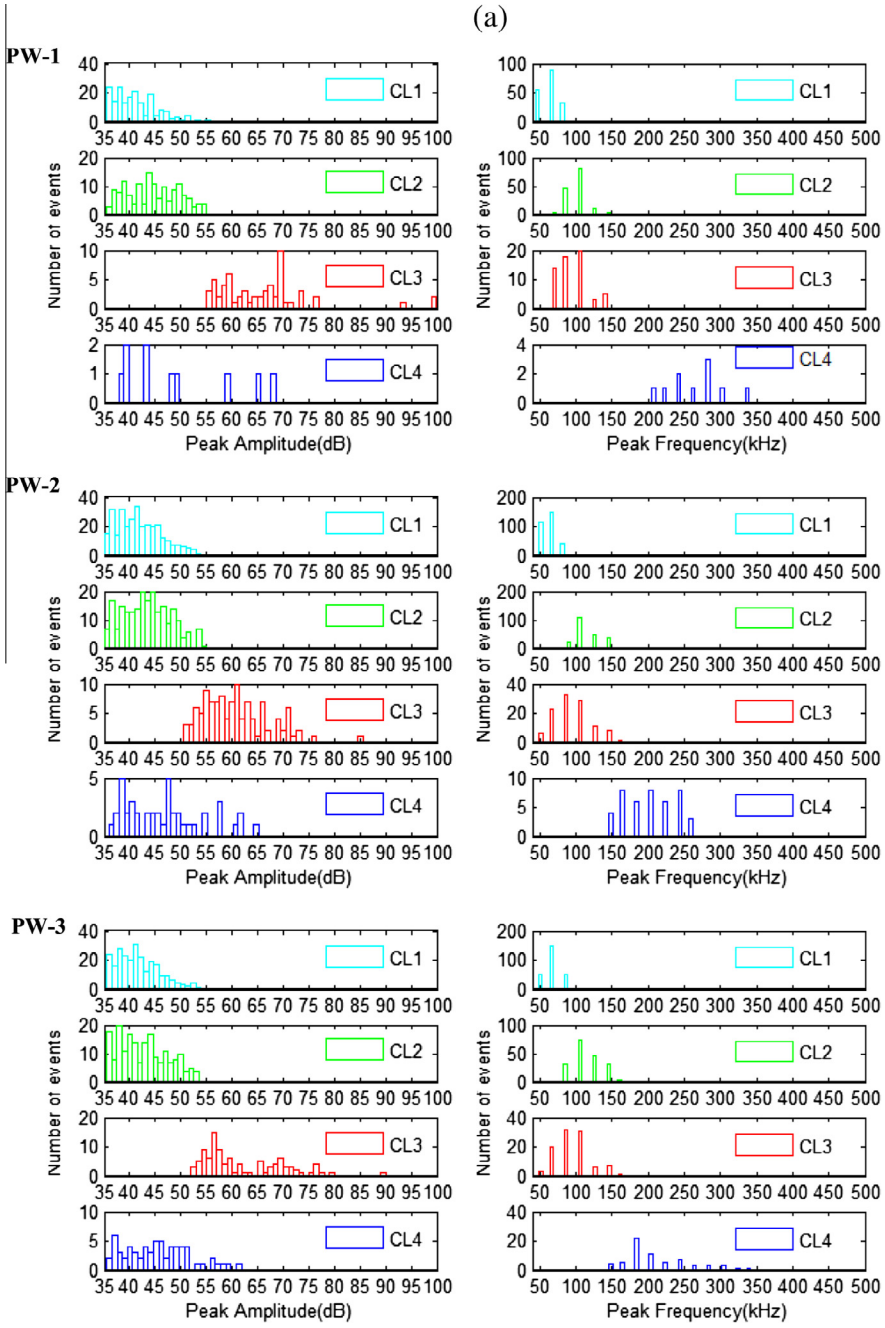

Fig. 12a. Peak amplitude distribution (left) and peak frequency distribution (right) of each cluster, PW specimens.

prominent damage in 3D woven composite in comparison with 2D woven composites, as discussed in detail in [21,22]. Fig. 5 shows the peak amplitude distribution and peak frequency distribution for all the specimens, respectively. It can be seen that for all the specimens of PW, they exhibit similar distribution, most events with peak amplitude range of 35–45 dB and peak frequency range of 50–150 kHz. They show similar conditions for the three 3W and 3F specimens.

3.3. Choice of AE parameters and clusters number

Fig. 6 shows the average Laplacian score of each AE feature for all the specimens. It is obvious that PA, E, PF, FCoG, RA value and WF have the value of Laplacian score more than 0.9 for 3 different tests, which means that they are good features and have the ability of clustering the AE data.

Fig. 7 compares the correlation of nine AE features with peak amplitude and peak frequency. It can be seen that energy and counts are highly correlated to PA; D and RT are less dependent on PA, and the correlation coefficients of PF, FCoG, RA value and WF with PA are around zero, which means that they are almost independent from PA. Weighted frequency is highly correlated to peak frequency, whereas frequency of centroid is less dependent. In summary, from correlation analysis, PA (or E), RT, PF, FCoG, IF, RF, CTP are independent. However, Laplacian score of D, RT are less than 0.9, thus they do not have the ability to cluster the AE signals.

In summary, the selected features for glass plain weave and 3D non-crimp textile composites are peak amplitude (PA), peak

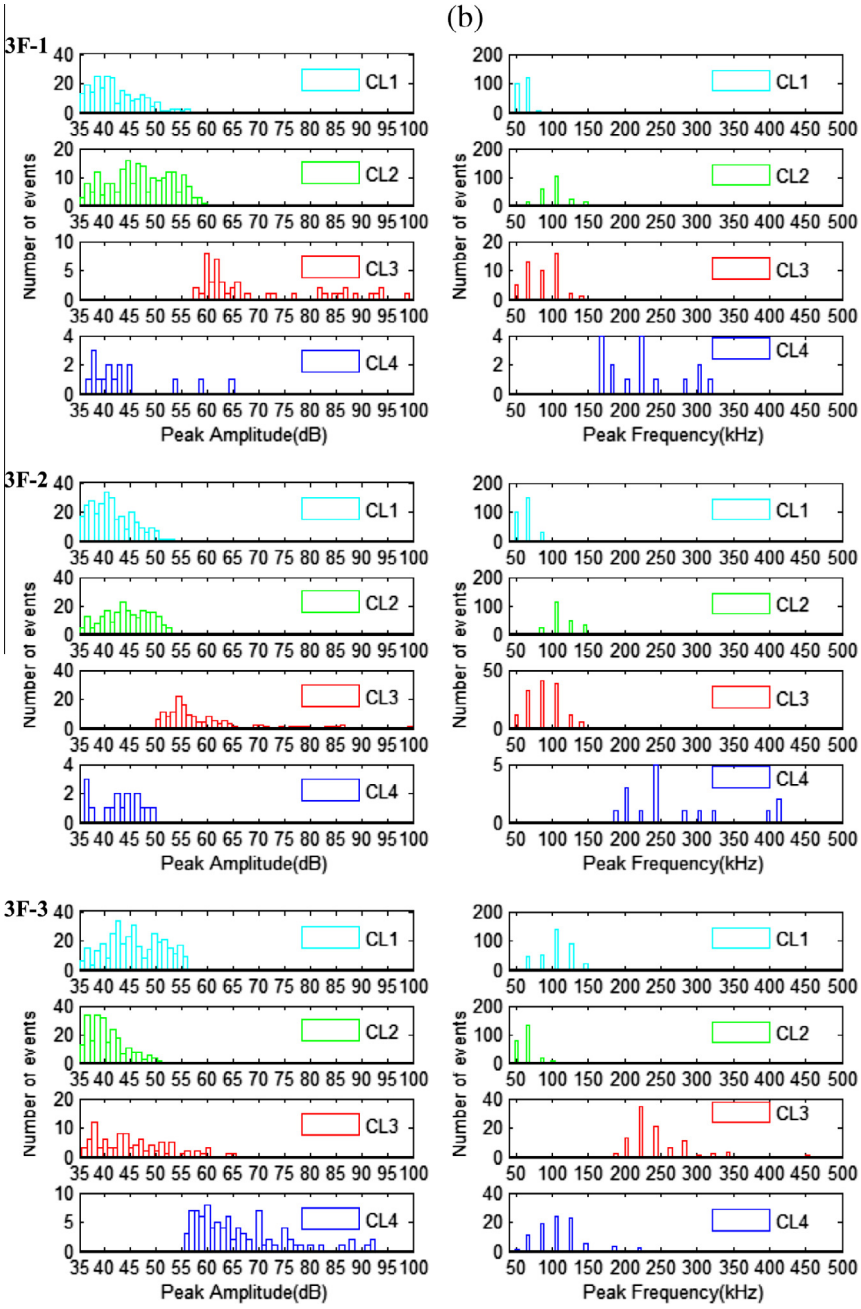

Fig. 12b. Peak amplitude distribution (left) and peak frequency distribution (right) of each cluster for 3W specimens.

frequency (PF), frequency of centroid (FCoG) and RA value, which are used as an initial set of AE descriptors in the clustering process.

The index of cluster evaluation used is Silhouette coefficient and Davies–Bouldin index defined in Eqs. (1) and (2) respectively. The number of cluster k is calculated using the range from 1 to 10 for PW, 3W and 3F data sets. The higher Silhouette coefficient and the lower Davies–Bouldin index means that better number of clusters. Fig. 8 shows that the optimal number of clusters for PW is four. The same is for 3F. For 3W the optimum is weak; however, choose of four as a number of clusters for this case also brings low values of Davies–Bouldin index and high values of the Silhouette coefficient. Therefore four is chosen as the cluster number for analysis of all the data sets. The cluster validity estimations for each 2D and 3D woven tests is summarized in Table 4. It can be seen that the Silhouette coefficient is good and acceptable ($0.6 < SC < 0.7$) for most tests according to [4], and low ($SC < 0.6$) for PW-1 and 3F-3. The DB index is less than 1, and proved the clustering quality for all tests.

3.4. Cluster analysis

Fig. 9 illustrates the percent variance and cumulative variance of each principal component. It is clear that the cumulative sum of the variances of the first two principal components (Pd1 and Pd2) explain roughly two-thirds of the total variability, so it is reasonable to limit the data presentation to these two components for better visualizing the AE data. The four principal components, defined by the PCA algorithm, are expressed as:

$$Pd1 = 2.0 \times PA + 4.7 \times PF - 0.6 \times RA + 3.2 \times FCoG \quad (3)$$

$$Pd2 = 5.6 \times PA - 1.7 \times PF - 0.9 \times RA - 0.7 \times FCoG \quad (4)$$

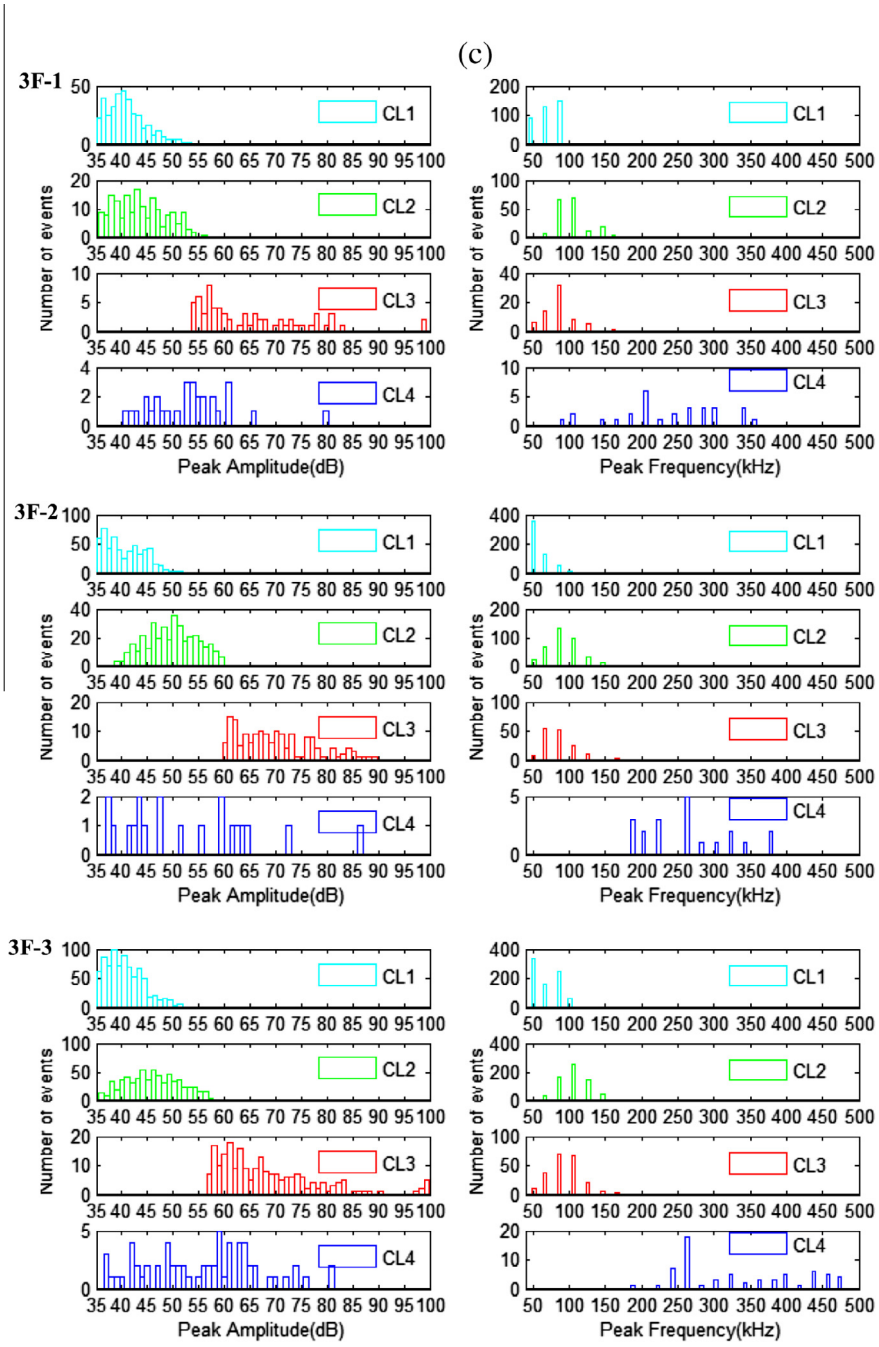

Fig. 12c. Peak amplitude distribution (left) and peak frequency distribution (right) of each cluster for 3F textile composites under tensile loading.

Table 5
Cluster bounds of PW and 3D textile composites.

Cluster bounds	PA (dB)	PF (kHz)
CL1	35–55	50–80
CL2	35–55	80–150
CL3	55–100	50–150
CL4	35–80	150–500

Fig. 10 presents the projection of the four clusters (designated for brevity CL1, CL2, CL3 and CL4) of AE events to two-dimensional plot by two principal components for PW, 3W and 3F specimens, respectively. It is obvious that AE signals are well separated by two components Pd1 and Pd2. Moreover, it is possible to further narrow the representative set of AE parameters. From the expressions for Pd1 and Pd2 (Eqs. (3) and (4)), it can be concluded that PA and PF are the most important AE parameters in the chosen set of four, as evidenced by the good separation of the clusters points in the space of these two parameters (Fig. 11).

3.5. Stability of cluster shapes and cluster bounds

Fig. 11 shows also that the shapes of the four clusters for all tests in this study are similar. CL1 have lower peak amplitude less and lower peak frequency, CL2 have lower peak amplitude like CL1 and slightly higher peak frequency, CL3 have higher peak

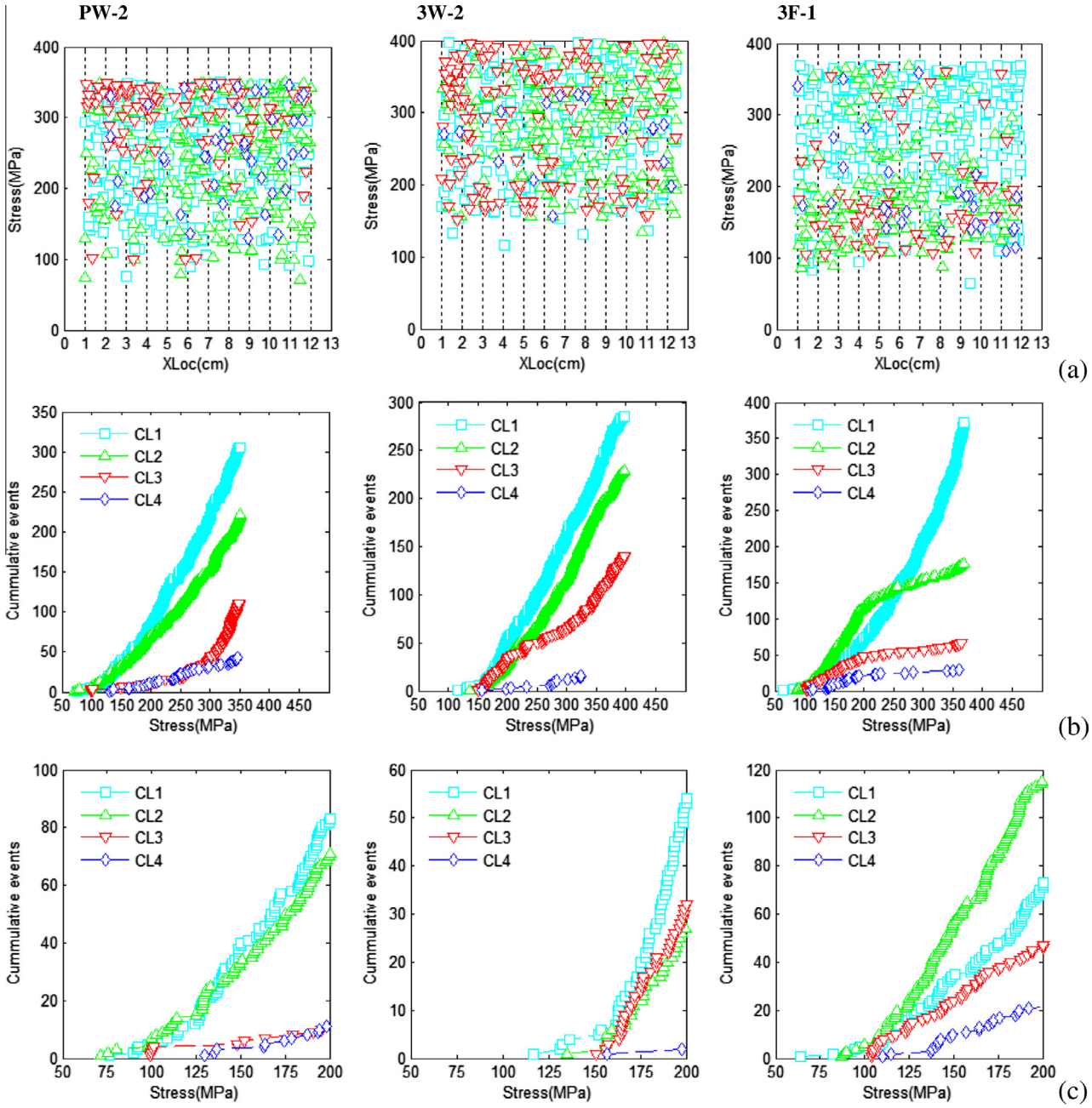

Fig. 13. Distribution of AE events in the clusters, PW-2, 3W-2, 3F-1: (a) by location of the event; (b) AE cumulative events vs stress, (c) AE cumulative events for stress <200 MPa.

amplitude and lower peak frequency and AE events in CL4 have broad peak amplitude range and higher peak frequency, almost more than 150 kHz. CL1 and CL2 are slightly overlapped, and CL3 and CL4 are better separated with the other two clusters. To better visualize the cluster boundaries, peak amplitude and peak frequency distribution of AE events for each PW, 3W and 3F woven specimen are shown in Figs. 12a–12c respectively. The similarity of the clusters for different data sets can be seen in these distributions.

The boundaries of the clusters can be evaluated as follows. Peak amplitude range of CL1 is between 35 and 55 dB, peak frequency less than 100 kHz, CL2 with peak amplitude same as CL1 and peak frequency of most events from 80 to 150 kHz, peak amplitude and peak frequency band of CL3 are about 55–100 dB and 50–150 kHz, and CL4 have broad amplitude range of 35–80 dB, and 150–500 kHz frequency range for most AE events. The cluster bounds are summarized in Table 5.

4. Discussion

In order to primarily correlate the resulted clusters with different damage mechanisms, four clusters were compared with peak amplitude distribution and peak frequency band which represents different damage mechanisms in glass fiber composite materials in literature [9,14,13,31]. CL1 and CL2 with amplitude range 35–55 dB have similar distribution with A-type signal as discussed in [11,14], which corresponds to matrix cracking. Similarly, CL3 with amplitude distribution 55–100 dB relates to fiber-matrix debonding (B-type signal) [14]. CL4 with higher peak frequency more than 150 kHz have similar amplitude distribution with D-type signal

which relates to delamination, and have broad amplitude range from 35 to 90 dB. High frequency can also be an indication of fiber breakage [13,15,16], although the threshold frequency values for AE events associated with fiber breakage, given by different authors, is in the range of 200,...,400 kHz [13,15,31].

Fig. 13(a)–(c) show AE events progression with increase of stress and their distribution by the location between AE sensors. Table 4 summarizes the percentage of events in each cluster for all tests.

For the representative PW-2 specimen, the four clusters consist of 44.9%, 33.3%, 16.3% and 6.3% events. From Fig. 13(a), it can be seen that CL1 starts early at about 60 MPa. Events in this cluster multiply fast and are distributed almost evenly between the sensors with certain concentrations in 3–5 cm and 11–12 cm range. CL2 starts early and grow faster than CL1, and have more events in 1–2 cm, 6–8 cm and 11–12 cm range. CL3 starts later at higher stress and grow slowly at first until the stress up to 280 MPa; after that the events multiply quite fast. The events start concentrating at the location 9–10 cm, but closer to failure more events are concentrated in the location 1–4 cm. CL4 starts at 120 MPa glow slowly first, but multiply fast after 250 MPa. Events are distributed almost evenly over the length of the specimen.

For the representative 3W-2 specimen, the AE events in each cluster occupy 42.3%, 34.1%, 21.2% and 2.4% respectively. From Fig. 13(b), it can be seen that CL1 starts at 110 MPa, later than in PW-2 specimen, CL1, CL2 and CL4 have the same distribution in the specimen as that of PW-2. Events in CL3 multiply fast at first and then slow down; they are concentrated in the location of 1–3 cm.

For the representative 3F-1 specimen (Fig. 13(c)), events in CL1 and CL4 have the same distribution as PW-2 and 3W-2, and the first clusters to be observed at the beginning of the AE activity are clusters 1 at around 50 MPa stress. Events of CL3 and CL4 were firstly observed at 100 MPa, all the events in CL2, CL3 and CL4 grow at the beginning of stress from 80 to 200 MPa, and then there are fewer events happened for these clusters.

5. Conclusion

The cluster analysis of AE during tensile loading of 2D and 3D orthogonally woven E-glass/epoxy composites, loaded in the direction of warp or weft fibers leads to the following conclusions valid for both types of the reinforcements and both warp and weft loading:

1. AE events can be discriminated in four clusters based on peak amplitude, peak frequency, frequency of centroid and RA value. Peak amplitude (PA) and peak frequency (PF) are the most important parameters in this discrimination. Moreover, for all the studied test variants the boundaries of the clusters in PA–PF coordinates are the same and given in Table 5. CL1 corresponds to low frequency low amplitude events, CL2 – moderate frequency, low amplitude, CL3 – low to moderate frequency, high amplitude and CL4 – high frequency.
2. The AE events in all the clusters are almost evenly distributed over the length of the specimen, with certain concentration of events at certain locations, indicating weak localization of the damage.
3. The order of the events initiation in the clusters is as follows

$$CL1 = CL2 < CL3 < CL4.$$

4. The order of the events number in the clusters during the whole test is as follows:

$$CL1 > CL2 > CL3 > CL4.$$

The correspondence between the AE events in the clusters and the damage mode can be hypothesized, based on literature data, as follows: CL1 and 2 – matrix cracking, CL3 – fiber/matrix debonding, CL4 –delamination and fiber breakage. This correspondence should be confirmed and detailed in the future work.

Acknowledgements

The research visit of L. Li to KU Leuven was funded by Chinese Scholarship Council and partially supported by FWO project G.0354.09. The raw AE data used in the present study was acquired by Guilia Gramellini during her Master thesis [23] research (supervisors V. Carvelli and S.V. Lomov). The help with Vallen AE system of Johan Vanhulst and useful discussions with Dr Helge Pfeiffer are acknowledged with gratitude.

References

[1] Johnson M. Waveform based clustering and classification of AE transients in composite laminates using principal component analysis. NDT E Int 2002;35:367–76.
[2] Pappas Y, Markopoulos Y, Kostopoulos V. Failure mechanisms analysis of 2D carbon/carbon using acoustic emission monitoring. NDT E Int 1998;31:157–63.
[3] Moevus M, Godin N, R'Mili M, Rouby D, Reynaud P, Fantozzi G, et al. Analysis of damage mechanisms and associated acoustic emission in two SiC_f/[Si–B–C] composites exhibiting different tensile behaviours. Part II: unsupervised acoustic emission data clustering. Compos Sci Technol 2008;68:1258–65.
[4] Gutkin R, Green C, Vangrattanachai S, Pinho S, Robinson P, Curtis P. On acoustic emission for failure investigation in CFRP: pattern recognition and peak frequency analyses. Mech Syst Signal Process 2011;25:1393–407.
[5] Sause M, Gribov A, Unwin A, Horn S. Pattern recognition approach to identify natural clusters of acoustic emission signals. Pattern Recognit Lett 2012;33:17–23.
[6] Sause M, Müller T, Horoschenkoff A, Horn S. Quantification of failure mechanisms in mode-I loading of fiber reinforced plastics utilizing acoustic emission analysis. Compos Sci Technol 2012;72:167–74.
[7] Bar HN, Bhat MR, Murthy CRL. Identification of failure modes in GFRP using PVDF sensors: ANN approach. Compos Struct 2004;65:231–7.
[8] Mechraoui S-E, Laksimi A, Benmedakhene S. Reliability of damage mechanism localisation by acoustic emission on glass/epoxy composite material plate. Compos Struct 2012;94:1483–94.
[9] Godin N, Huguet S, Gaertner R, Salmon L. Clustering of acoustic emission signals collected during tensile tests on unidirectional glass/polyester composite using supervised and unsupervised classifiers. Ndt E Int 2004;37:253–64.
[10] Huguet S, Godin N, Gaertner R, Salmon L, Villard D. Use of acoustic emission to identify damage modes in glass fibre reinforced polyester. Compos Sci Technol 2002;62:1433–44.
[11] Godin N, Huguet S, Gaertner R. Integration of the Kohonen's self-organising map and k-means algorithm for the segmentation of the AE data collected during tensile tests on cross-ply composites. NDT E Int 2005;38:299–309.
[12] De Oliveira R, Marques A. Health monitoring of FRP using acoustic emission and artificial neural networks. Comput Struct 2008;86:367–73.
[13] Arumugam V, Kumar B, Santulli C, Stanley AJ. Effect of fiber orientation in unidirectional glass epoxy laminate using acoustic emission monitoring. Acta Metall Sin (English Lett) 2011;24:351–64.
[14] Marec A, Thomas J-H, El Guerjouma R. Damage characterization of polymer-based composite materials: multivariable analysis and wavelet transform for clustering acoustic emission data. Mech Syst Signal Process 2008;22:1441–64.
[15] Pashmforoush F, Fotouhi M, Ahmadi M. Acoustic emission-based damage classification of glass/polyester composites using harmony search k-means algorithm. J Reinf Plast Compos 2012;31:671–80.
[16] Arumugam V, Kumar CS, Santulli C, Sarasini F, Stanley AJ. A global method for the identification of failure modes in fiberglass using acoustic emission. J Test Eval 2011;39:1.
[17] Barre S, Benzeggagh M. On the use of acoustic emission to investigate damage mechanisms in glass-fibre-reinforced polypropylene. Compos Sci Technol 1994;52:369–76.
[18] Ely TM, Hill E. Longitudinal splitting and fiber breakage characterization in graphite epoxy using acoustic emission data. Mater Eval 1995;53:288–94.
[19] Suzuki M, Nakanishi H, Iwamoto M, Jinen E. Application of static fracture mechanisms to fatigue fracture behavior of class A-SMC composite. In: Japan-US conference on composite materials, 4th, Washington, DC; 1989. p. 297–306.
[20] Carvelli V, Gramellini G, Lomov SV, Bogdanovich AE, Mungalov DD, Verpoest I. Fatigue behavior of non-crimp 3D orthogonal weave and multi-layer plain weave E-glass reinforced composites. Compos Sci Technol 2010;70:2068–76.

[21] Lomov SV, Bogdanovich AE, Ivanov DS, Mungalov D, Karahan M, Verpoest I. A comparative study of tensile properties of non-crimp 3D orthogonal weave and multi-layer plain weave E-glass composites. Part 1: materials, methods and principal results. Compos A: Appl Sci Manuf 2009;40:1134–43.
[22] Ivanov DS, Lomov SV, Bogdanovich AE, Karahan M, Verpoest I. A comparative study of tensile properties of non-crimp 3D orthogonal weave and multi-layer plain weave E-glass composites. Part 2: comprehensive experimental results. Compos A: Appl Sci Manuf 2009;40:1144–57.
[23] Gramellini G. Comparative study of tensile fatigue behavior and damage development of non-crimp 3D orthogonal weave and multilateral plain weave E-glass composites. Politecnico di Milano; 2009.
[24] Alelyani S, Tang J, Liu H. Feature selection for clustering: a review. In: Aggarwal Charu, Reddy Chandan, editors. Data clustering: algorithms and applications. CRC Press; 2013.
[25] He X, Cai D, Niyogi P. Laplacian score for feature selection. Adv Neural Inf Process Syst 2005:p–14.
[26] Cai D, Zhang C, He X. Unsupervised feature selection for multi-cluster data. Proceedings of the 16th ACM SIGKDD international conference on knowledge discovery and data mining. ACM; 2010. p. 333–42.
[27] Jolliffe I. Principal component analysis. Wiley Online Library; 2005.
[28] Arthur D, Vassilvitskii S. K-means++: the advantages of careful seeding. In: Proceedings of the eighteenth annual ACM-SIAM symposium on discrete algorithms: Society for Industrial and Applied Mathematics; 2007. p. 1027–35.
[29] Maulik U, Bandyopadhyay S. Performance evaluation of some clustering algorithms and validity indices. IEEE Trans Pattern Anal Mach Intell 2002;24:1650–4.
[30] Wang G, Wang Z, Chen W, Zhuang J. Classification of surface EMG signals using optimal wavelet packet method based on Davies–Bouldin criterion. Med Biol Eng Comput 2006;44:865–72.
[31] Suzuki M, Nakanishi H, Iwamoto M, Jinen E, Maekawa Z, Koike K, et al. Study of fracture mechanism of class A-SMC based on acoustic emission method. J Soc Mater Sci Jpn 1987;36:229–35.